Nanofluid Electrodes made of Hybrid Graphene-Polyoxometalate Nanocomposites for Dual Energy Storage in Novel Flow Cells.

Deepak P. Dubal[a,], Daniel Rueda-Garcia,[a] Pedro Gomez-Romero[a,b**]*

[a]Catalan Institute of Nanoscience and Nanotechnology (ICN2), CSIC and The Barcelona Institute of Science and Technology, Campus UAB, Bellaterra, 08193 Barcelona, Spain

[b]Consejo Superior de Investigaciones Científicas (CSIC), Spain

CORRESPONDING AUTHOR FOOTNOTE

Dr. Deepak Dubal, and Prof. Pedro Gomez-Romero

Tel.: +349373609/+345929950 Fax: +345929951

E-mail:* dubaldeepak2@gmail.com (D. Dubal),

**pedro.gomez@icn2.cat (P. Gomez-Romero). LEAD CONTACT

Highlights

First hybrid flowing supercapacitor demonstrated

Stable Reduced Graphene Oxide/Polyoxometalate nanofluids prepared

Active materials perform as well as in solid electrodes in a highly efficient flowing cell

The Bigger Picture

Batteries and supercapacitors feature very different electrochemistries (faradaic and capacitive, respectively) and distinct energy/power profiles. Batteries lay at the high-energy / low-power corner whereas supercaps feature high power but relatively low energy. It is only natural to try to combine battery and supercap materials and electrodes in order to get the best of each type of device, and a great and growing number of laboratories are presently exploring that approach by designing hybrid materials with combined faradaic and capacitive energy-storage mechanisms.

But energy storage is not limited to portable or mobile applications. There is a whole category of batteries addressing stationary applications, in which Redox Flow Batteries (RFBs) constitute the leading technology. Very recently flow analogs of supercapacitor cells have been proposed and tested. This paper is a first example of a hybrid (faradaic + capacitive) flowing cell which could show a way to get the best of batteries and supercapacitors in the flowing realm.

Summary

The first example of a hybrid electroactive nanofluid (HENFs) combining capacitive and faradaic energy storage mechanism in a single fluid material is presented. This liquid electrode is composed of reduced graphene oxide and polyoxometalates (rGO-POMs) forming a stable nanocomposite for electrochemical energy storage in novel Nanofluid Flow Cells. Two graphene based hybrid materials (rGO-phosphomolybdate, rGO-PMo_{12} and rGO-phosphotungstate, rGO-PW_{12}) were synthesized and dispersed with the aid of a surfactant in 1 M H_2SO_4 aqueous

electrolyte to yield highly stable hybrid electroactive nanofluids (HENFs) of low viscosity which were tested in a home-made flow cell under static and continuous flowing conditions. Remarkably, even low concentration rGO-POMs HENFs (0.025 wt%) exhibited high specific capacitances of 273 F/g(rGO-PW_{12}) and 305 F/g(rGO-PMo_{12}) with high specific energy and specific power. Moreover, rGO-POM HENFs show excellent cycling stability (~95 %) as well as coulombic efficiency (~97 %) after 2000 cycles. Thus, rGO-POM HENFs effectively behave as real liquid electrodes with excellent properties, demonstrating the application of HENFs for dual energy storage in a new generation of Nanofluid Flow Cells.

Introduction

The development of large-scale stationary energy-storage systems is vitally important in order to develop smart grids and fully harness sustainable energy resources, including solar and wind.[1] Thus, current research on energy storage is thriving. Traditional technologies are creatively revisited and novel energy storage approaches are being quickly developed including those related to post-Li-ion batteries, supercapacitors and electrochemical flow cells. [2 3] Among them, electrochemical flow cells such as redox flow batteries (RFB) are raising their hands as promising electrical energy storage devices for stationary applications. However, the limited solubility of the electroactive species used in conventional flow battery solutions limits in turn their energy density. Increasing energy density without sacrificing cost, could make of flow cells practical systems not only to store intermittent renewable energy but even to feed Electric Vehicles (EVs).[4] Several groundbreaking investigations on electrochemical flow cells have been recently reported in order to simultaneously achieve the demands of high energy and high power,[1] but none of them involved the use of nanofluids. *At this right time, we posed the question "could we develop hybrid electroactive nanofluids which could be used as liquid electrodes in energy storage flow cells?" Our first results, reported here, gave us a positive answer*

Nanofluids are homogeneous dispersions of nanoparticles in conventional base fluids which constitute an emerging type of unique liquid materials within the field of Nanoscience and Nanotechnology. Several applications of nanofluids have been explored with very special prominence on thermal properties and heat-transfer applications.[5] However, they have never been proposed as possible electroactive materials. A few recent investigations have suggested the use of thick slurries as electrodes for energy storage in flow cells. For instance, Gogotsi et al.[6] reported an electrochemical flow capacitor (EFC) using a flowable carbon slurry improving

upon the concept introduced by Kastening et al,.[7] Very recently we have also reported graphene nanofluids featuring ultrafast charge transfer.[8] Yet, all of these recent reports were on flowing materials with a purely capacitive storage mechanism

We present here the first examples of the use of hybrid electroactive nanofluids (HENFs) which could be used as improved energy density liquid electrode in flow electrochemical cells by combining redox as well as capacitive double-layer mechanisms.

We first prepared solid nanocomposite hybrid materials based on redox-active polyoxometalates (POMs) supported on reduced Graphene Oxide nanosheets (rGO), the latter providing a double-layer capacitive storage mechanism. In particular we used phosphomolybdate (PMo_{12}) and phosphotungstate (PW_{12}) clusters.

In order to prepare the corresponding HENFs, rGO-POMs hybrid materials were dispersed in different proportions in aqueous electrolyte (1 M H_2SO_4) to be directly used as liquid electrodes for charge storage in flow cells. Interestingly, this type of hybrid nanofluids combines the high-energy storage capabilities of redox POMs clusters with the high power provided by the electric double layer (EDL) mechanism of reduced graphene oxide (rGO). The HENFs reported here were able to store electricity through both mechanisms, as the parent solid-electrode supercapacitors, except that in the present case the electrode is a liquid, stored externally and flowing through a flow electrochemical cell.

Results

In order to confirm the effective anchoring of POMs on the surface of 3D open porous rGO nanosheets, multiple morphological characterizations were carried out. Figure 1 (a, b) presents SEM images of rGO-PMo_{12} and rGO-PW_{12} hybrid materials with the corresponding elements mapping and EDAX spectra. It is interesting to note that, rGO preserves its 3D open porous structure even after heavy deposition of PW_{12} and PMo_{12} clusters, which is highly beneficial to enhance the electron transport while keeping good ionic conductivity within each

solid particle. EDS mapping and elemental analyses of rGO-POM hybrid samples evidently confirm the homogeneous and efficient anchoring of PW_{12} and PMo_{12} clusters onto the rGO nanosheets. Figure 2 (a-c) shows STEM images of rGO, rGO-PW_{12} and rGO-PMo_{12} samples, respectively. It is clearly seen that the surface of rGO nanosheets is blank and free from tiny spots (Figure 2 a) while in great contrast the surface of rGO-POMs hybrids is abundantly decorated with nanometer-sized PW_{12} and PMo_{12} dots (Figure 2 b-c) (see also EDS mapping with STEM in S.I. S1). It is also interesting to note that the POM clusters are evenly distributed at a strictly molecular level without any agglomeration.

It is very important to note the utterly dispersed nature of the electroactive centers in this hybrid material. These POM clusters have a stable structure and size (1nm diameter), with all twelve W or Mo moieties on the surface of the cluster (there is no “bulk”). Therefore, the present hybrid configuration is ideal for fast (diffusion-free) faradaic processes added to the inherently fast capacitive polarization of graphene. Furthermore, it should be noted that rGO-PW_{12} and rGO-PMo_{12} exhibit high surface areas of 237 m^2/g and 231 m^2/g, respectively (S.I. S2). The slight decrease in the active surface for rGO-PW_{12} is attributed to the inclusion of the PW_{12} nanoparticles, which contribute heavily to the total mass of the hybrid. Even with this slight decrease the specific BET surface area of rGO-PW_{12} is considerably larger than many recently reported carbon/metal oxide hybrid materials.[9-10]

Figure 2 (d-f) shows core level XPS spectra of C1s, Mo3d and W4f, respectively. The detection of Mo3d peaks at 232.3 eV ($Mo3d_{3/2}$) and 235.4 eV ($Mo3d_{5/2}$) unambiguously confirms the presence of PMo_{12} in rGO-PMo_{12} hybrid with a predominance of Mo(VI) oxidation state (Figure 2 e).[11, 12] while core-level W4f spectrum shows two peaks at 37.54 eV ($W4f_{5/2}$) and 35.4 eV ($W4f_{7/2}$) with spin-orbit splitting of 2.14 eV (with a peak ratio 4:3). The position and shape of these peaks are representative of W atoms with an oxidation state of W(VI) further confirming the presence of PW_{12} in rGO-PW_{12} hybrid (Figure 2 f).[13, 14]

The electrochemical characterization of rGO-POMs HENFs was carried out both under static and continuous flow conditions using a specially designed flow cell (Figure 3 (a-b)). Hybrid Electroactive Nanofluids (HENFs) of rGO-POMs were prepared by direct mixing of different proportions of rGO-POMs (rGO-PMo_{12} or rGO-PW_{12}) (0.025 %, 0.1 % and 0.4 %) in 1 M H_2SO_4 aqueous solution (where, H_2SO_4 acts as an electrolyte). These dispersions of rGO-POMs HENFs were directly used as liquid electrodes in electrochemical flow cells (see Figure 3 (c)).

The rheological properties of rGO-POMs HENFs were measured under variable shear rates ranging from 25/s to 150/s. In the present study, the base fluid composed of water with surfactant (0.5 % triton X-100) and electrolyte (1 M H_2SO_4) showed Newtonian behaviour with a viscosity of approximately 1 mPa s, in the shear rate range of 25-150 /s at room temperature (25°C), essentially identical to the theoretical value of water (1 mPa s).[15] The viscosities of rGO-POMs HENFs of different concentrations with shear rate were determined and are plotted in Figure 3 (d). There are two kinds of viscosity variations for rGO-POMs HENFs are observed with increase in shear rate: Newtonian and shear-thinning behaviors. As seen in Figure 3 (d), the viscosity of rGO-POMs HENFs decreases slightly with shear rate, showing the shear-thinning behavior. It is further seen that with an increase in the concentration of solid nanoparticles the viscosities of the rGO-POMs HENFs increase but are in all cases between 1.2 to 1.8 mPa s, very close to that of water (1 mPa s).[16] These low values are far better than those for carbon-slurry based electrodes (ca. 2000 mPa s).[6, 17] These results undoubtedly ascertain the suitability of rGO-POMs HENFs to be used as liquid electrodes in electrochemical flow cells without any flowing or clogging problems.

Electrochemical performance of rGO-POMs Hybrid Electroactive Nanofluids (HENFs)

Before exploring their final application in flow cells, we tested the electrochemical properties of rGO and rGO-POMs HENFs in conventional three-electrode cells comprising glassy carbon, platinum wire and Ag/AgCl as working, counter and reference electrodes,

respectively. Figure 4 shows CV curves of rGO and rGO-POMs HENFs at 60 mV/s scan rate. The CV curve for rGO nanofluid exhibits a featureless rectangular shape characteristic of double layer capacitive mechanism whereas CV curves for rGO-POMs hybrid nanofluids show quasi-rectangular capacitive behavior but with well-defined redox peaks on top, confirming both EDL and faradaic charge storing mechanism. This test definitely confirmed our successful preparation of hybrid electroactive nanofluids. CV curves for rGO and rGO-POMs HENFs at different scan rates are shown in Figure S3 (see S.I. S3).

In order to demonstrate the practical application of these rGO-POMs HENFs, their electrochemical performance was tested in flow cells under static and flowing conditions using the cell described above. Figure 5 (a-b) shows the Cyclic polarization curves of symmetric rGO-PW_{12} and rGO-PMo_{12} HENFs cells at different scanning rates under static conditions. It is worth noting that, the shape of CV curves for rGO-POMs HENFs is different than that for rGO nanofluid with extensive improved current densities (S.I. S4). Furthermore, CV curves up to very high scan rate of 5 V/s (5000 mV/s) for rGO-POMs HENFs were recorded (S.I. S5). Most remarkably, the rectangular CV shape was maintained even at a very high scan rate of 5000 mV/s, indicating rGO-POMs HENFs exhibit excellent rate capabilities as needed for high-power supercapacitors. This is an extremely fast scan rate, much greater than values reported to have been used in CV measurements of any capacitive flow cell.[18-20] It should be noted that the shape of CV curves becomes more and more rectangular with increase in scan rate. This indicates an increasingly important relative contribution of capacitive (Double Layer) energy storage vs. pseudocapacitive (faradaic) energy storage at high rates. Again, this could be expected for any conventional solid carbon based hybrid electrode, given the slower rates of redox reactions and electron transfer processes when compared with electrophysical double layer polarization.

The specific capacitances of the cell for rGO-POMs HENFs were calculated from the CV curves for 0.025 % concentration at different scanning rates (S.I.6). As expected, specific

capacitances decrease gradually with increasing scan rate (Figure 5 c). Maximum specific capacitance values of 273 F/g(rGO-PW_{12}) and 306 F/g(rGO-PMo_{12}) were obtained for 0.025 % rGO-POM HENFs at a scan rate of 5 mV/s. Here again, in order to store that amount of charge on rGO-POMs HENFs within the flow cell, the rGO flakes must be electrically connected to the external load via a conductive pathway. Unlike conventional supercapacitors in which solid film electrodes benefit from well-defined fixed conduction paths, our cell utilizes a 'liquid electrode' in which charge must percolate through a dynamic network of conductive particles. Figure 5 (d) shows the capacity retention with scan rate. It is observed that about 12-14 % of specific capacitance is retained for rGO-POMs HENFs as scan rate increases from 5 mV/s to 200 mV/s, suggesting good rate capability of the material in flow cell. The values of specific capacitances obtained in this work are very much comparable or even higher than the values reported for thicker carbon slurries as well as solid carbon-POM based electrodes. For instance, Presser et al.[6] prepared a thick carbon slurry of carbide-derived carbon powder obtained from titanium carbide (TiC: CDC) and 1 M Na_2SO_4 with compositions of 3:1 and 4:1 (electrolyte: carbon by mass). The highest specific capacitance reported for toothpaste-like TiC:CDC slurry (3:1, electrolyte: carbon) was 109 F/g at the scan rate of 2 mV/s. Furthermore, Zhang et al.[18] reported a specific capacitance of 154 F/g at 2 mV/s in 1 M H_2SO_4 for a thick slurry of porous carbon spheres with concentration ranging from 16 wt% to 23 wt%. Moreover, our recent investigation on activated carbon-PW_{12} and Activated carbon-PMo_{12} solid electrodes showed a specific capacitance of 254 F/g and 183 F/g, respectively.[19, 20] Thus, our present study provides most impressive preliminary data supporting the use of hybrid electroactive nanofluids in general and of rGO-POMs HENFs in particular for energy storage applications.

The electrochemical performance of rGO-POMs HENFs was further studied by galvanostatic charge/discharge test in static conditions as shown in Figure 6 (a-b). The shapes of charge-discharge curves are not symmetrically triangular showing a great contribution from the redox species of POMs molecular clusters. The maximum values of specific capacitance

obtained for the 0.025 % rGO-POMs HENFs were 207.7 F/g(rGO-PW_{12}) and 222.8 F/g(rGO-PMo_{12}) at current density of 4 A/g, respectively. This capacitance corresponds to specific energy values of 28.85 Wh/kg(rGO-PW_{12}) and 30.95 Wh/kg(rGO-PMo_{12}) and specific power of 2-8 kW/kg(rGO-POMs) as shown in Figure 6 (c). The values obtained for rGO-POMs HENFs are remarkably higher than those measured for rGO nanofluids (13.1 Wh/kg(rGO)) which can be due to the synergetic combination of rGO and POMs redox clusters. Moreover, the values of specific energy are significantly higher than those previously reported for slurries (for example, 5.6-8.2 Wh/kg for carbon beads slurry[17]). Furthermore, the galvanostatic charge/discharge cycling performance was tested at different current densities for 2000 cycles. The rGO-POMs HENFs were found to be remarkably stable, with cycle efficiencies greater than about 94-95 % after 2000 charge/discharge cycles (Figure 6 d). This confirms the stable attachment of the POMs redox clusters to the graphene sheets.

Figure 7 (a-b) shows a series of chronoamperometry experiments carried out for rGO-PW_{12} and rGO-PMo_{12} HENFs under static conditions. Initially, the cell was completely discharged for a period of 15 min and then charged to different potentials such as 0.4, 0.6, 0.8 and 1.0 V. While charging was associated with additional leakage current, the integration of the discharge current *versus* time plot directly yields the charge for a given cell voltage (as plotted in Figure 7 c). The flow cell capacitances were calculated by simply dividing by the cell voltage and are displayed in Figure 7 (d). When compensating for the leakage current, this translates into device capacitances of 0.70-0.72 F for rGO-POMs HENFs. Moreover, the coulombic efficiency of the rGO-POMs nanofluid cell was found to be 95.3 % (a large value since we did include the leakage current).

Energy storage of rGO-POMs HENFs under flowing condition

As a final test for the use of our nanofluids in flow cells, we tested the electrochemical properties of rGO-POMs HENFs under continuous flow conditions. Indeed, it is interesting to

note that the shape of the CV curves slightly changes for the different flow rates used, which may be due to the migration of the redox electroactive clusters (see Figure 7 (e-f)). However, the current under the curve slightly increases with increase in flow rate from 0 to10 ml/min but then remains constant for flow rates > 10 ml/min. This initial increase in current density may be attributed to the flow of fresh rGO-POMs nanoparticles taking part in charge storage. However, at high flow rates, and under the experimental conditions used, the residence time for rGO-POMs nanoparticles in the flow channels will eventually be insufficient for completing the expected redox reactions of all the dispersed material, consequently leading to the saturation in current density. In addition, CV curves of rGO-POMs at different flowing rates for different scan rates are presented (see S.I. 7).

Conclusions

Our present investigation has established the first successful example of the possible use of hybrid electroactive nanofluids for energy storage in electrochemical flow cells. In particular our work provides proof of this breakthrough concept by demonstrating the use of hybrid rGO-POMs nanofluids for dual energy storage through a hybrid (faradaic-capacitive) mechanism.

The results certainly confirmed that these rGO-POMs HENFs electrodes exhibit excellent electrochemical performances, including high capacitance and energy density as well as high rate performance and long cycle life. Most strikingly, our study shows full electrochemical utilization of both components of the hybrid (rGO and POMs) in the bulk nanofluid, even at very fast rates, thus showing effective charge percolation in a material that behaves as a true liquid electrode. This discovery promotes the application of rGO-POMs HENFs as truly flowing electrodes for Electrochemical Flow Cells. Further investigations are already in progress concerning both improved engineering design and improved active materials. That combination should lead to efficient, low-cost and scalable flow cells based on Electroactive Nanofluids

(ENFs) which could help to improve grid efficiency and accelerate widespread implementation of levered renewable energy sources.

Methods

Synthesis of reduced graphene oxide (rGO) and rGO-POM nanofluids

Graphene oxide (GO) was synthesized from natural graphite using the modified Hummers method. Briefly, 5 g $NaNO_3$ and 225 ml H_2SO_4 were added to 5 g graphite and stirred for 30 min in an ice bath. 25 g $KMnO_4$ was added to the resulting solution, and then the solution was stirred at 50 °C for 2 h. 500 ml deionized water and 30 ml H_2O_2 (35%) were then slowly added to the solution, and the solution was washed with dilute HCl. Further, the GO product was washed again with 500 ml concentrated HCl (37%). The reduced graphene oxide was prepared by high temperature treatment of the GO sample at 800 °C.

In second step, we have prepared graphene based hybrid materials with phosphomolybdate (rGO-PMO_{12}) and phosphotungstate (rGO-PW_{12}). Briefly, 0.25 gm of rGO was dispersed in 100 ml of deionized water with probe sonicator (of power 1500 watt) for 1 hr. Later, 10 mM of phosphomolybdic acid ($H_3PMo_{12}O_{40}\cdot 3H_2O$, ($PMo_{12}$)) and 10 mM of phosphotungstic acid ($H_3PW_{12}O_{40}\cdot 3H_2O$, ($PW_{12}$)) were added in above pre-sonicated rGO solutions. These suspensions were further sonicated (bath sonicator 200 watt) for 5 hr. and kept at room temperature for next 24 hrs. Afterwards, the product was filtered off and dried in vacuum oven at 80 °C for overnight.

Hybrid electroactive nanofluids (HENFs) were prepared by direct mixing of rGO-POMs (rGO-PMo_{12} or rGO-PW_{12}) in the base fluid. In this analysis base fluid is deionized water with 1 M H_2SO_4. HENFs with different concentrations were prepared by mixing 0.025, 0.1 and 0.4 wt%

of rGO-PMOs in 1 M H_2SO_4 aqueous solution. In order to get stable suspension, 0.5 wt% of surfactant (triton X-100) is added and the mixture is kept in an ultrasonic bath up to 2 h. This suspension is further used as flowable electrode in electrochemical flow cell.

Flow cell assembly

The cell body (7 cm × 6 cm × 1 cm) was made of two stainless-steel plates (acting as current collectors) with a carved serpentine flow channel 5 mm wide and 5 mm deep. The cell compartments were separated by a polyvinylidene fluoride (PVDF) membrane (Durapore®; Merck Millipore, Germany) and oil paper was used as a gasket providing airtight sealing. The contact area between the ion-permeable membrane and the flow electrode was 12.7 cm^2. Finally, the cell was designed with the high level of flow control required for prototype testing in order to meet the expectations for a large-scale EFC device. Thus, dual (back and forth) automated flow control of peristaltic pumps for each, positive and negative compartments was implemented. This home-made flow cell, alike conventional flow battery cells does allow for the use of nanofluids but not the flow of slurries (at least not an energy-efficient flow).

Characterization techniques

Surface morphological analysis of rGO sample was carried out by scanning electron microscopy (FEI Quanta 650F Environmental SEM). TEM images were obtained with a field emission gun transmission electron microscope (Tecnai G2 F20 S-TWIN HR(S) TEM, FEI). X-ray photoelectron analyses were carried out by X-ray photoelectron spectroscopy (XPS, SPECS Germany, PHOIBOS 150). N_2 adsorption/desorption was determined by Brunauer-Emmett-Teller (BET) measurements using Micromeritics instrument (Data Master V4.00Q, Serial#:2000/2400). Rheological measurements were carried out with Rheometer HAAKE RheoStress RS600 from Thermo Electron Corporation. Electrochemical characterizations such

as cyclic voltammetry (CV), galvanostatic charge/discharge (chronopotentiometry, CP), Chronoamperometry (CA), electrochemical impedance measurements of rGO nanofluid symmetric cell were carried out with Biologic SP200 potentiostat.

Acknowledgements

Partial funding from MINECO-FEDER (MAT2015-68394-R) and AGAUR (NESTOR 2014_SGR_1505) are gratefully acknowledged. Authors appreciate the award to DPD with the support of the Secretary for Universities and Research of the Ministry of Economy and Knowledge of the Government of Catalonia and the Co-fund programme of the Marie Curie Actions of the 7th R&D Framework Programme of the European Union". ICN2 acknowledges support from the Severo Ochoa Program (MINECO, Grant SEV-2013-0295).

References

[1] Dunn, B. Kamath, H. Tarascon, J. M. Electrical energy storage for the grid: A battery of choices. *Science*, **334**, 928-935 (2011).

[2] Dubal, D. P. Ayyad, O. Ruiz, V. Gomez-Romero, P. Hybrid energy storage: the merging of battery and supercapacitor chemistries. *Chem. Soc. Rev.* **44**, 1777-1790 (2015).

[3] Chakrabarti M.H. *et al.* Application of carbon materials in redox flow batteries, *J. Power Sources*, **253**, 150-166 (2014).

[4] Leung, P. et al. Progress in redox flow batteries, remaining challenges and their applications in energy storage. *RSC Adv.*, **2**, 10125-10156 (2012).

[5] Taylor, R. *J.* Small particles, big impacts: a review of the diverse applications of nanofluids*. J. Appl. Phys.* **113**, 011301 (2013).

[6] Presser, V. *et al.* The electrochemical flow capacitor: A new concept for rapid energy storage and recovery. *Adv. Energy Mater*. **2**, 895-902 (2012).

[7] Kastening, B. Boinowitz, T. Heins, M. Design of a slurry electrode reactor system. *J. Appl. Electrochem.* **27**, 147-152 (1997).

[8] Dubal, D. P. and Gomez-Romero, P. Electroactive Graphene Nanofluids for Fast Energy Storage. *2D-Materials*, **3**, 031004 (2016).

[9] Ji, Y. Huang, L. Hu, J. Streb, C. Song, Y. F. Polyoxometalate-functionalized nanocarbon materials for energy conversion, energy storage and sensor systems, *Energy Environ. Sci.*, **8**, 776-789 (2015)

[10] Chen, H. Y. *et al.* A novel SWCNT-polyoxometalate nanohybrid material as an electrode for electrochemical supercapacitors, *Nanoscale*, **7**, 7934-7941 (2015).

[11] Ma, A. *et. al.* Graphene and polyoxometalate synergistically enhance electro-catalysis of Pd toward formic acid electro-oxidation. *J. Electrochem. Soc.*, **161,** F1224-F1230 (2014)

[12] Bajwa, G., Genovese, M. Lian, K. Multilayer polyoxometalates-carbon nanotube

composites for electrochemical capacitors. *ECS J. Sol. State Sci. Tech.*, **2,** M3046-M3050 (2013)

[13] Barreca, D. *et al.* A Study of Nanophase Tungsten Oxides Thin Films by XPS. *Surf. Sci. Spectra*, **8**, 258 (2001)

[14] Weinhardt, L. *et al.* Electronic surface level positions of WO_3 thin films for photoelectrochemical hydrogen production. *J. Phys. Chem. C,* **112**, 3078-3082 (2008).

[15] Pastoriza-Gallego, M.J. Casanova, C. Legido, J. L. Pineiro, M. M. CuO in water nanofluid: Influence of particle size and polydispersity on volumetric behaviour and viscosity. *Fluid Phase Equilibr.* **300**, 188-196 (2011).

[16] Hong, R.Y. Rheological properties of water-based Fe_3O_4 ferrofluids. *Chem. Eng. Sci.* **62**, 5912-5924 (2007).

[17] Campos, J. W. et al. Investigation of carbon materials for use as a flowable electrode in electrochemical flow capacitors. *Electrochim. Acta* **98**, 123-130 (2013).

[18] Zhang, C. *et al.* Highly porous carbon spheres for electrochemical capacitors and capacitive flowable suspension electrodes. *Carbon*, **77**, 155-164 (2014).

[19] Suarez-Guevara, J. Ruiz, V. Gomez-Romero, P. Hybrid energy storage: high voltage aqueous supercapacitors based on activated carbon-phosphotungstate hybrid materials. *J. Mater. Chem. A*, **2**, 1014-1021 (2014)

[20] Ruiz, V. Suarez-Guevara, J. Gomez-Romero, P. Hybrid electrodes based on polyoxometalates-carbon materials for electrochemical supercapacitors. *Electrochem. Commun.* **24**, 35-38 (2012)

Figure captions

Figure 1 SEM images of (a) rGO-PW_{12} and (b) rGO-PMo_{12} hybrid materials with corresponding mapping images and EDX elemental spectrum which suggests mooring of POM clusters to rGO nanosheets showing characteristic molybdenum and tungsten peaks in the spectrum

Figure 2 (a-c) Scanning transmission electron micrographs (STEM) of rGO, rGO-PW_{12}, rGO-PMo_{12} hybrid, respectively (d-f) core-level C1s, Mo*3d* and W*4f* spectra of rGO-PMo_{12} and rGO-PW_{12} material

Figure 3 (a) Schematic diagram of the flow cell setup used in this work in which charged and discharged nanofluids are stored in separate containers. Two peristaltic pumps with automatic control of flow direction and flow rate were used, (b) Digital photograph of our home-made flow cell which consists of stainless-steel current collectors (7 cm × 6 cm × 1 cm) with a carved serpentine, polyvinylidene fluoride (PVDF) membrane as a separator and oil paper as a gasket enclosed together using hard plastic plates and screws, (c) Actual photographs of rGO, rGO-PMo_{12} and rGO-PW_{12} HENFs (0.025 % in 1 M H_2SO_4 aqueous solution) showing stable and uniform sols, (d) The viscosity of rGO, rGO-PMo_{12} and rGO-PW_{12} HENFs of different concentrations with shear rate.

Figure 4 CV curves of rGO and rGO-POMs HENFs at 60 mV/s scan rate with conventional three electrode set-up comprising glassy carbon, platinum wire and Ag/AgCl as working, counter and reference electrodes, respectively.

Figure 5 (a-b) CV curves of rGO-PW_{12} and rGO-PMo_{12} HENFs of 0.025 % concentration at different scanning rates, respectively (c) Variation of specific capacitance with scan rates for rGO-POMs HENFs, (d) Plot of capacity retention with scan rate for rGO-POMs HENFs.

Figure 6 (a-b) Galvanostatic charge-discharge curves for rGO-PW_{12} and rGO-PMo_{12} HENFs of 0.025 % at different current densities in static condition, (b) Plot of specific energy versus specific power in Ragone plot for rGO, rGO-PW_{12} and rGO-PMo_{12} in flow cell (d) Galvanostatic charge/discharge cycling test for rGO-POMs HENFs of 0.025 % at different current densities for 2000 cycles.

Figure 7 (a-b) Chronoamperometry test for rGO-PW_{12} and rGO-PMo_{12} HENFs (0.025 %) under static condition at different applied voltages such as 0.4, 0.6, 0.8 and 1.0 V which shows high coulombic efficiency of 95.3 % when charged to a cell potential of 1.0 V and subsequently discharged to 0 V, (c) Plot of charge extracted by integrating discharge curves with given potential, (d) Plot of device capacitance versus given potential for rGO-PMOs HENFs in flow cell, (e-f) CV curves of rGO-PW_{12} and rGO-PMo_{12} for different flow rates at scan rate of 200 mV/s, respectively.

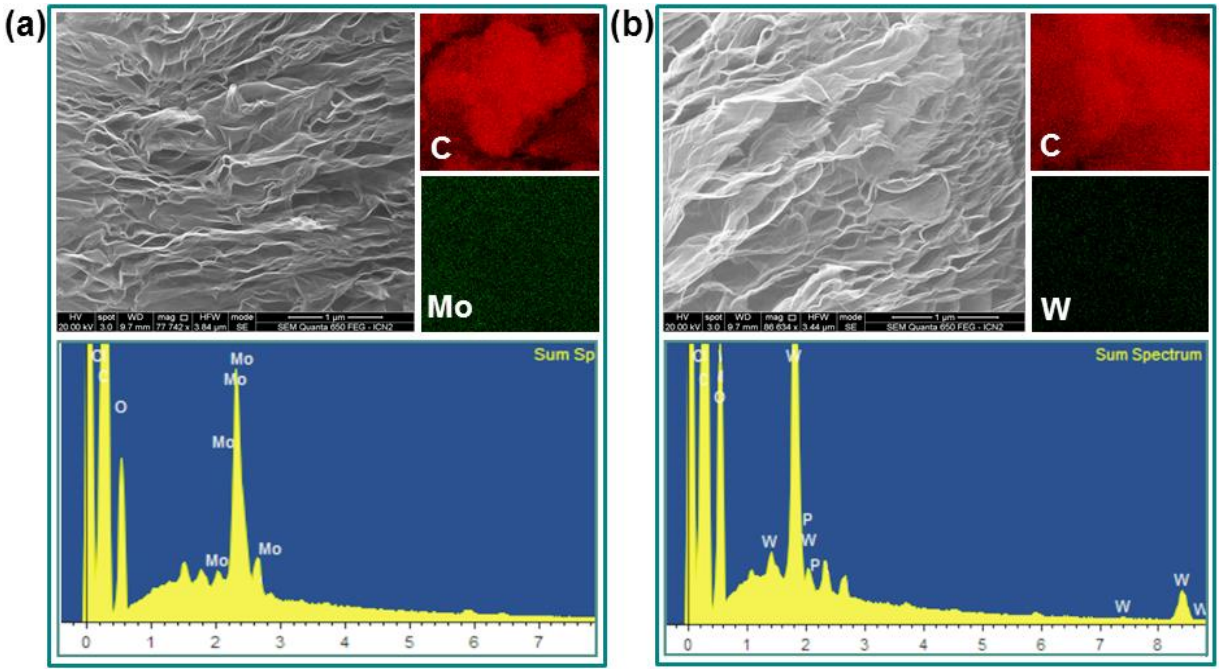
(a)
C
Mo
Sum Sp
O
Mo
Mo
Mo
Mo
Mo
0 1 2 3 4 5 6 7
(b)
C
W
Sum Spectrum
O
W
P
W
P
W
W
W
0 1 2 3 4 5 6 7 8

Figure 1

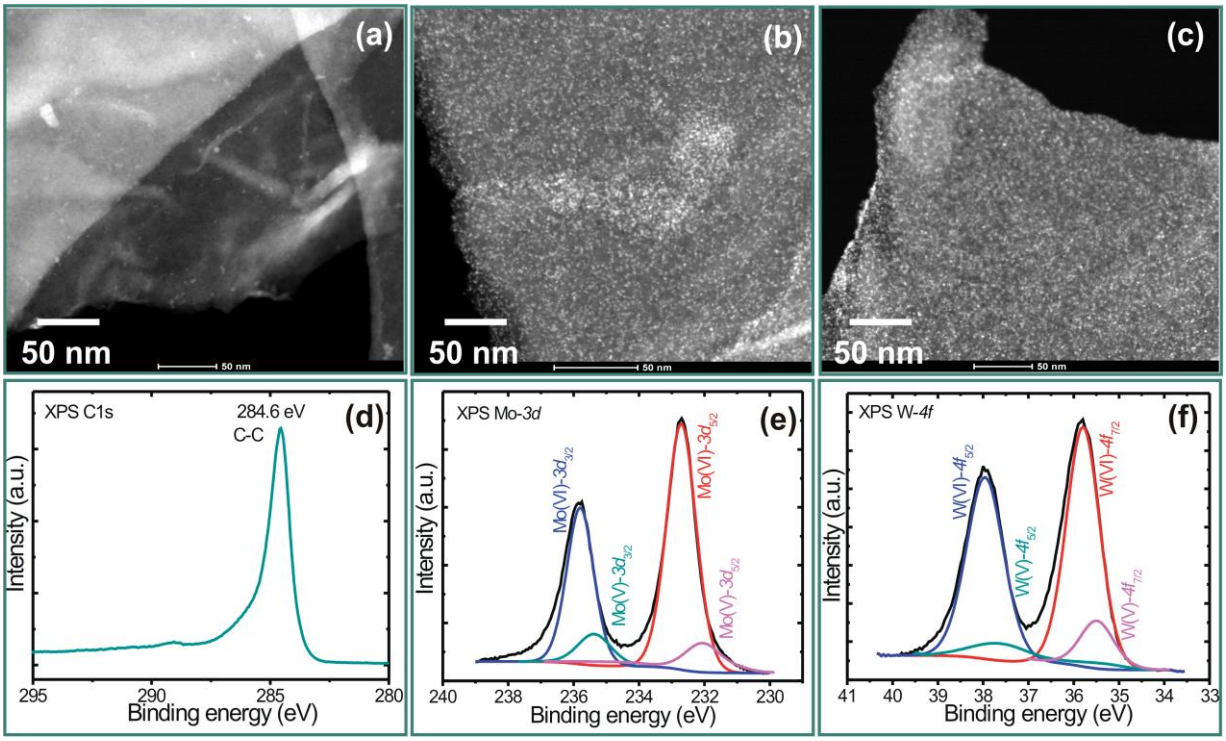
(a)
50 nm
(b)
50 nm
(c)
50 nm
XPS C1s
284.6 eV
C-C
(d)
Intensity (a.u.)
295
290
285
280
Binding energy (eV)
XPS Mo-3d
(e)
Mo(VI)-3d3/2
Mo(V)-3d3/2
Mo(VI)-3d5/2
Mo(V)-3d5/2
Intensity (a.u.)
240
238
236
234
232
230
Binding energy (eV)
XPS W-4f
(f)
W(VI)-4f5/2
W(V)-4f5/2
W(VI)-4f7/2
W(V)-4f7/2
Intensity (a.u.)
41
40
39
38
37
36
35
34
33
Binding energy (eV)

Figure 2

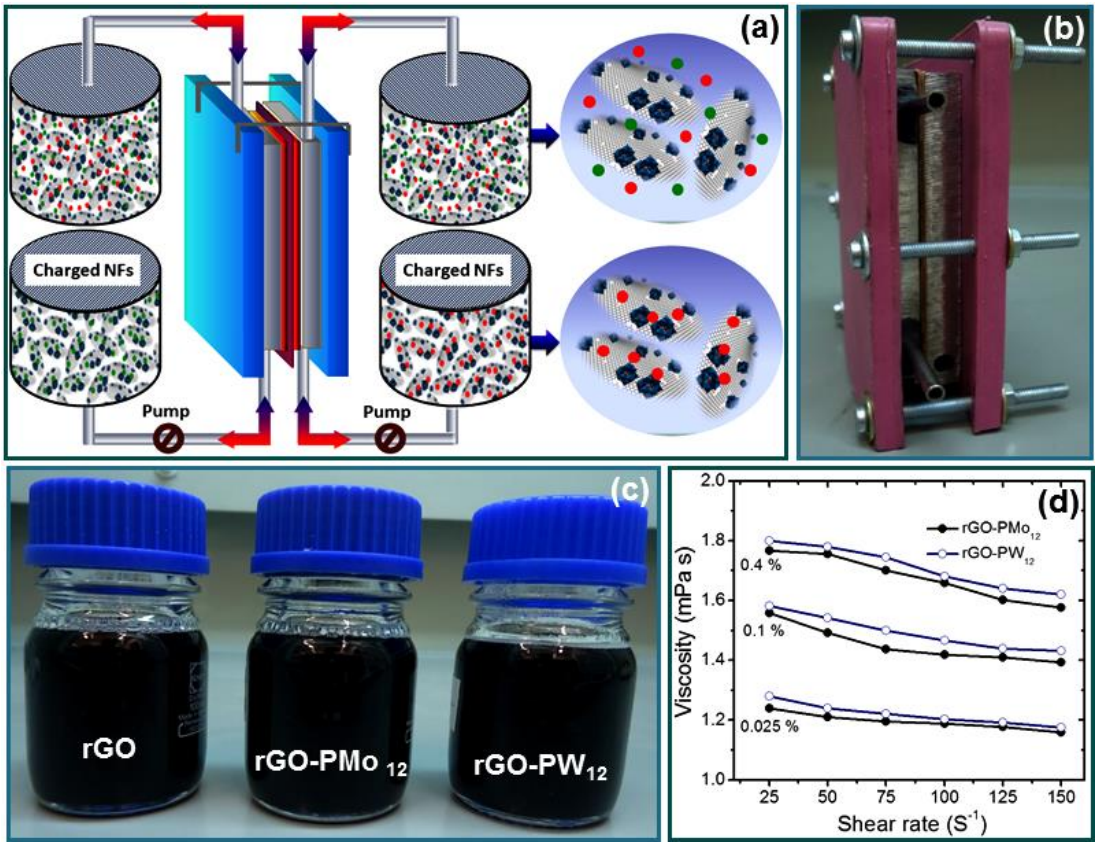
(a)
Charged NFs
Charged NFs
Pump
Pump
(b)
(c)
rGO
rGO-PMo 12
rGO-PW12
(d)
rGO-PMo12
rGO-PW12
0.4 %
0.1 %
0.025 %
Viscosity (mPa s)
Shear rate (S-1)
2.0
1.8
1.6
1.4
1.2
1.0
25
50
75
100
125
150

Figure 3

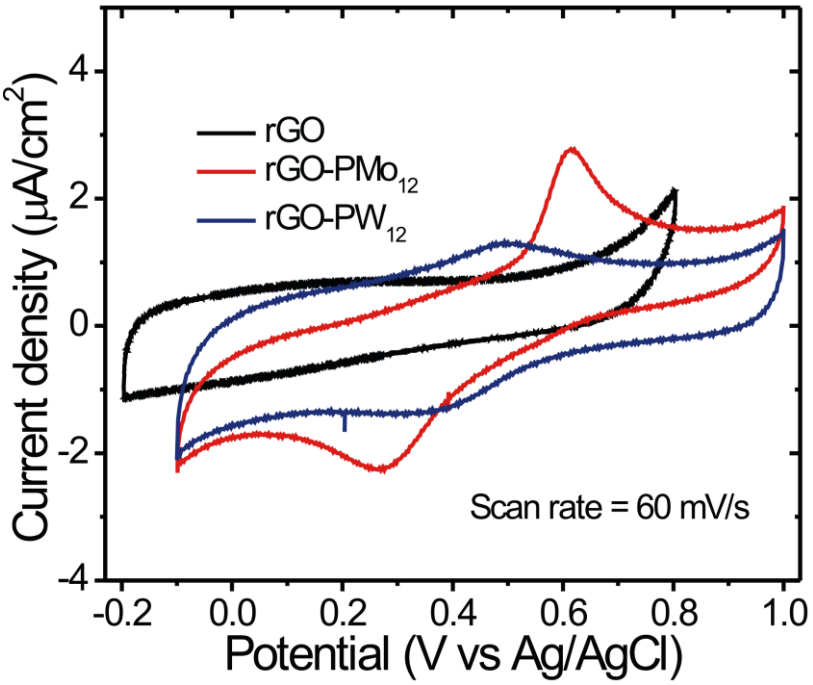
rGO
rGO-PMo12
rGO-PW12
Scan rate = 60 mV/s
Current density (μA/cm2)
Potential (V vs Ag/AgCl)
4
2
0
-2
-4
-0.2
0.0
0.2
0.4
0.6
0.8
1.0

Figure 4

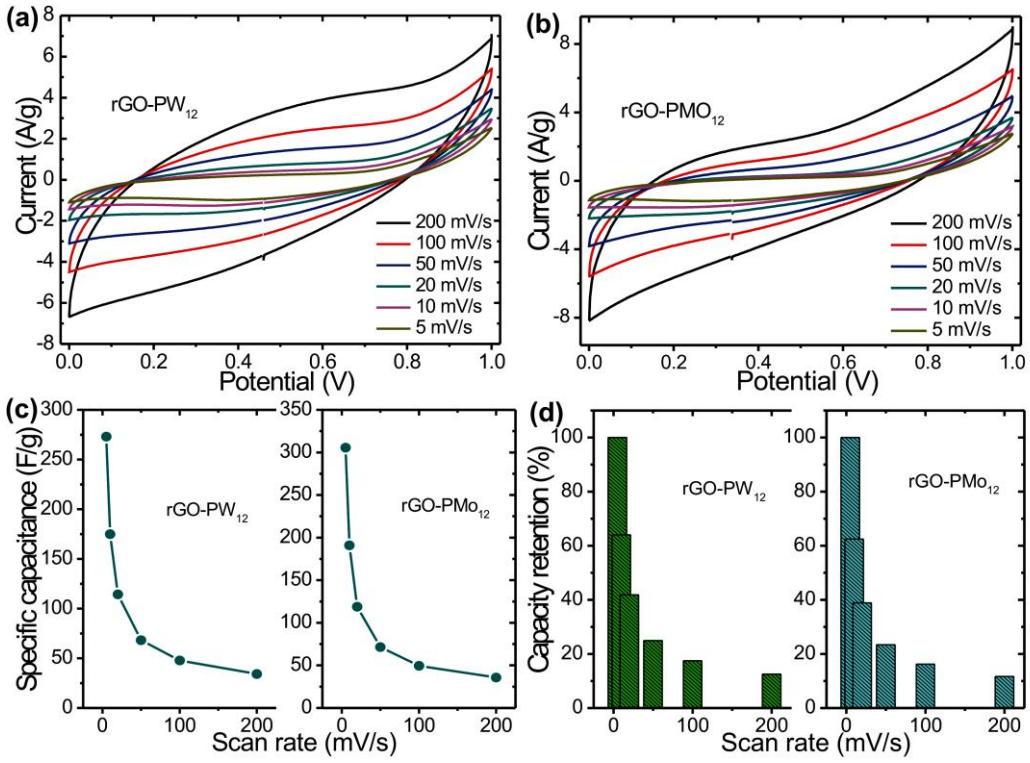
(a)
rGO-PW12
Current (A/g)
Potential (V)
200 mV/s
100 mV/s
50 mV/s
20 mV/s
10 mV/s
5 mV/s
(b)
rGO-PMO12
Current (A/g)
Potential (V)
200 mV/s
100 mV/s
50 mV/s
20 mV/s
10 mV/s
5 mV/s
(c)
Specific capacitance (F/g)
rGO-PW12
rGO-PMo12
Scan rate (mV/s)
(d)
Capacity retention (%)
rGO-PW12
rGO-PMo12
Scan rate (mV/s)

Figure 5

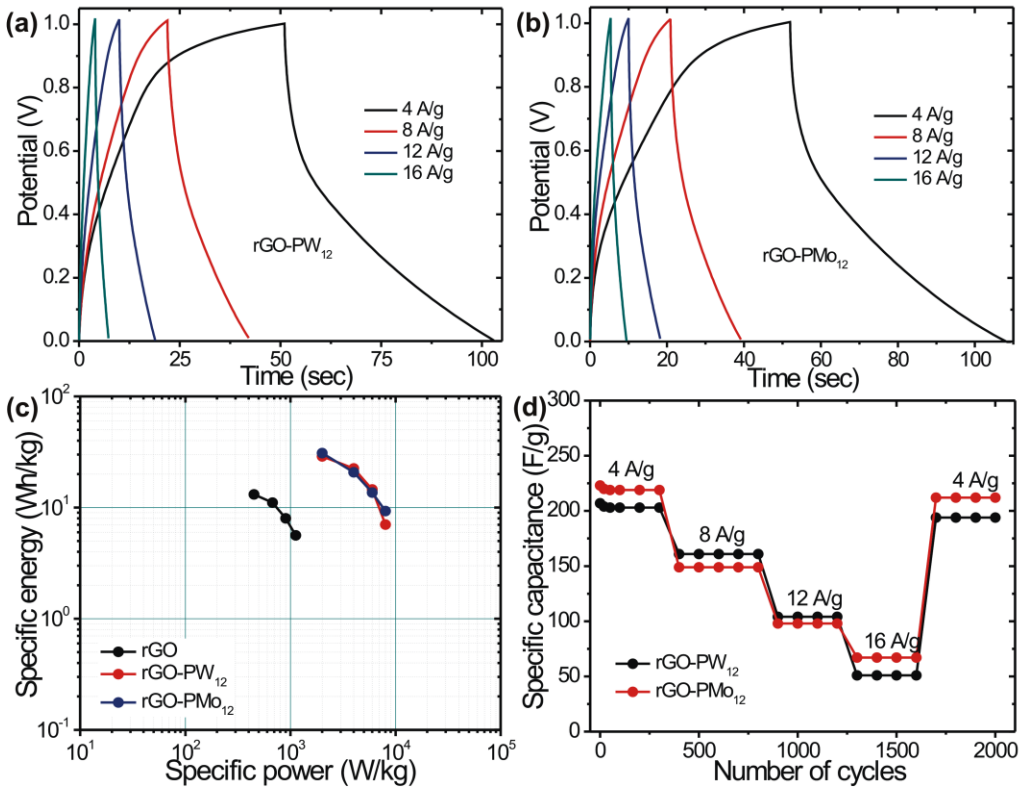
(a)
Potential (V)
Time (sec)
4 A/g
8 A/g
12 A/g
16 A/g
rGO-PW12
(b)
Potential (V)
Time (sec)
4 A/g
8 A/g
12 A/g
16 A/g
rGO-PMo12
(c)
Specific energy (Wh/kg)
Specific power (W/kg)
rGO
rGO-PW12
rGO-PMo12
(d)
Specific capacitance (F/g)
Number of cycles
4 A/g
8 A/g
12 A/g
16 A/g
4 A/g
rGO-PW12
rGO-PMo12

Figure 6

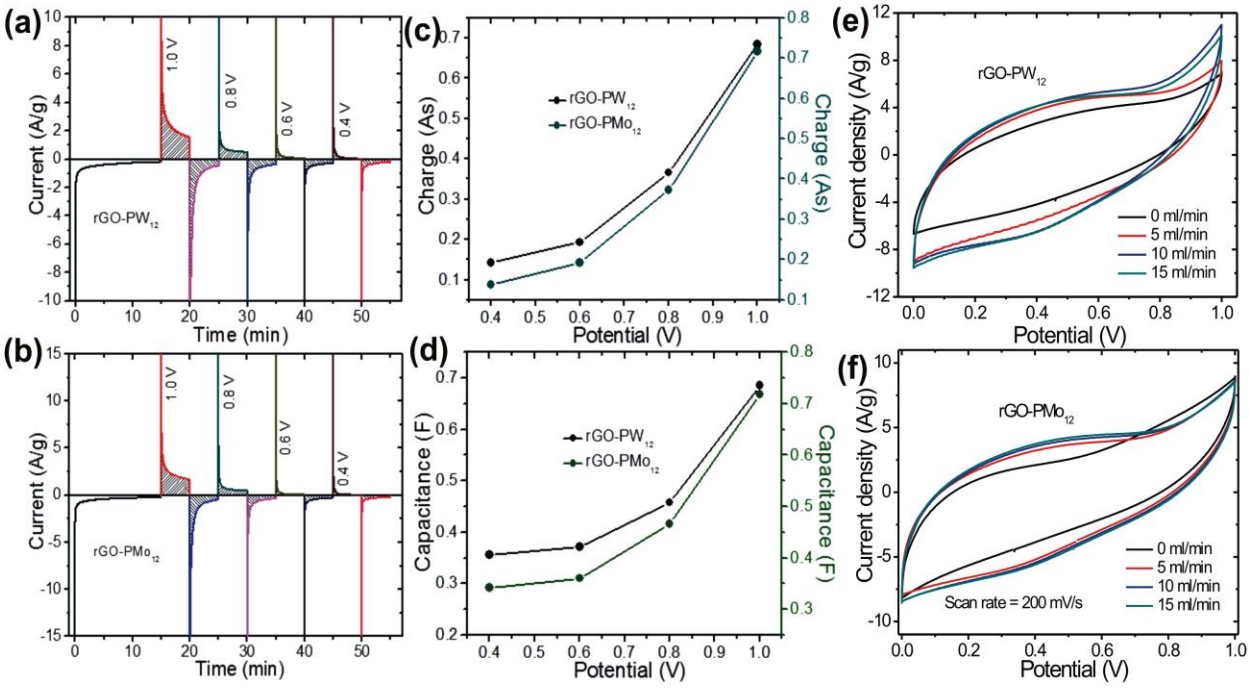
(a)
Current (A/g)
Time (min)
1.0 V
0.8 V
0.6 V
0.4 V
rGO-PW12
(b)
Current (A/g)
Time (min)
1.0 V
0.8 V
0.6 V
0.4 V
rGO-PMo12
(c)
Charge (As)
Potential (V)
rGO-PW12
rGO-PMo12
(d)
Capacitance (F)
Potential (V)
rGO-PW12
rGO-PMo12
(e)
Current density (A/g)
Potential (V)
rGO-PW12
0 ml/min
5 ml/min
10 ml/min
15 ml/min
(f)
Current density (A/g)
Potential (V)
rGO-PMo12
Scan rate = 200 mV/s
0 ml/min
5 ml/min
10 ml/min
15 ml/min

Figure 7

Author contributions

D. P. D. and P. G. R. designed the experiments, analyzed the data and wrote the manuscript. D. P. D. carried out synthesis and characterization of materials and nanofluids. DRG helped with some electrochemical tests. D. P. D. and P. G. R. designed the whole experimental flow cell set-up and carried out electrochemical measurements. To the preparation and reviewing manuscript, all authors contributed equally.

Additional information

Competing financial interests: The authors declare no competing financial interests.

Suplemental Text and Figures

Nanofluid Electrodes made of Hybrid Graphene-Polyoxometalate Nanocomposites for Dual Energy Storage in Novel Flow Cells.

Deepak P. Dubal[a,], Daniel Rueda-Garcia,[a] Pedro Gomez-Romero[a,b]***

Supporting information S1

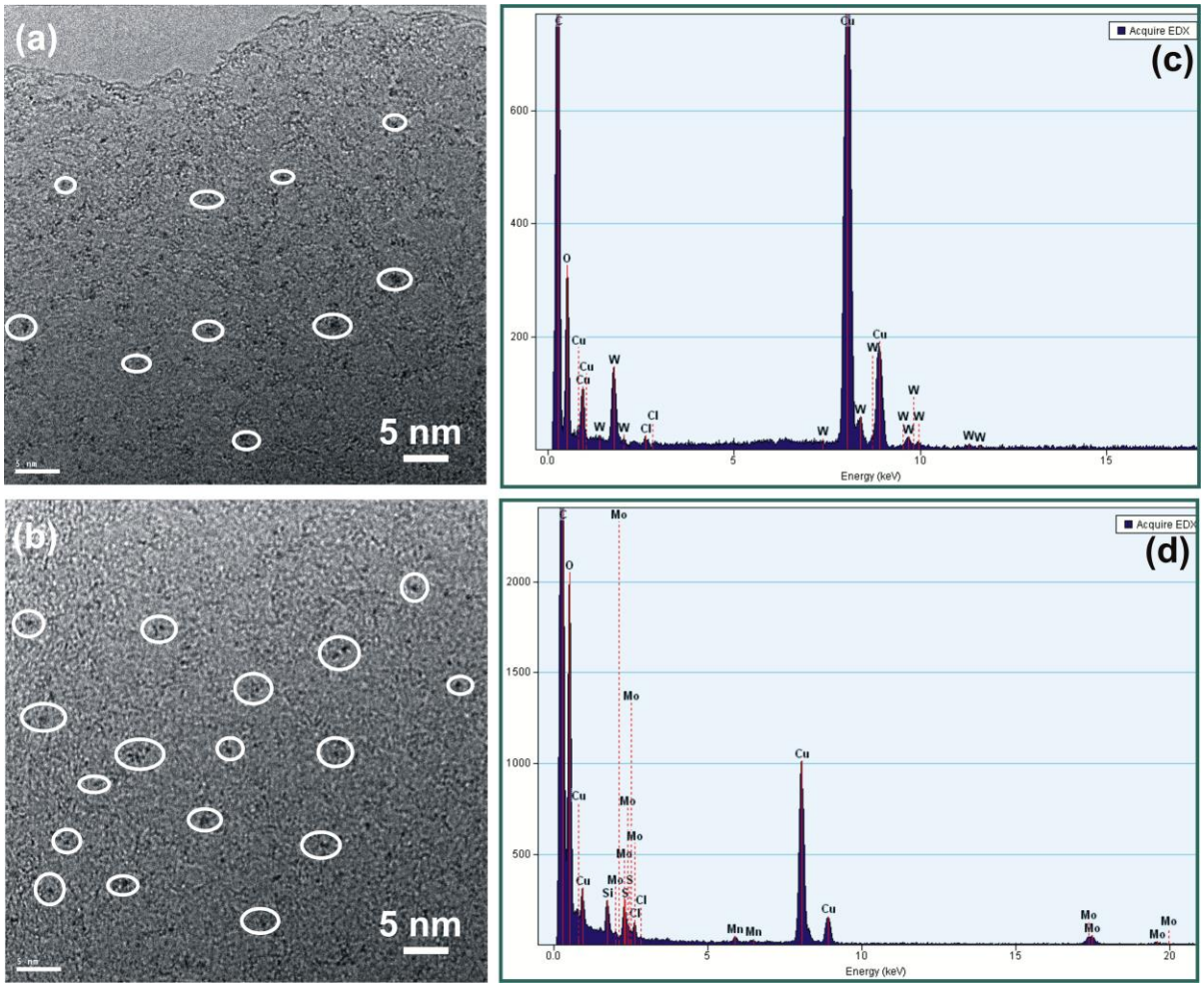

Figure S1 (a, b) shows HRTEM images of rGO-PW_{12} and rGO-PMo_{12} hybrid, respectively. As seen in Figure, few parts are highlighted with circles to realize the presence of PW_{12} and PMo_{12} clusters however that is not only the part covered by POMs. (c, d) EDS spectra of rGO-PW_{12} and rGO-PMo_{12} hybrid materials. EDX analysis explicitly confirmed the mooring of PW_{12} and PMo_{12} clusters to rGO nanosheets showing characteristic tungsten and molybdenum peaks in the spectrum.

Supporting information S2

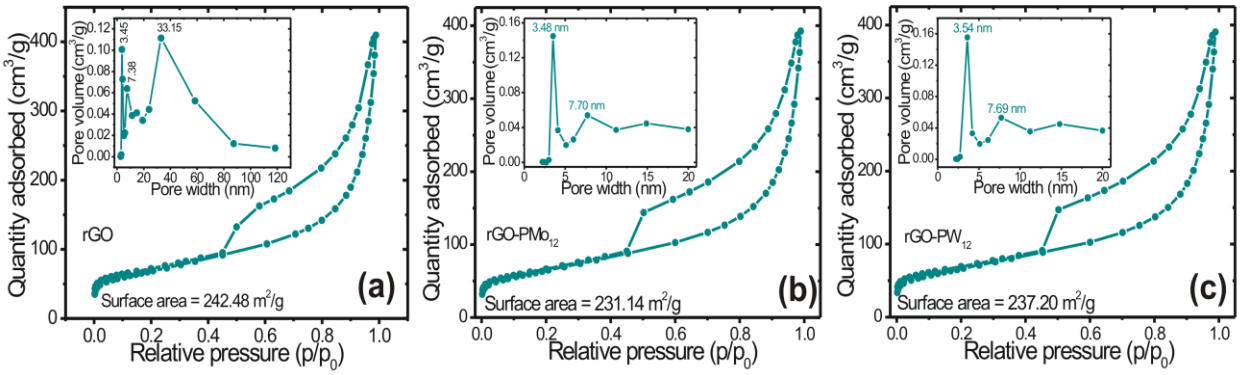

Figure S2 (a-c) Nitrogen adsorption-desorption curves and the corresponding pore size distribution plots for rGO, rGO-PMo_{12} and rGO-PW_{12} samples, respectively. The shape of the hysteresis loop is characteristic of mesoporous materials. BET analyses of these data showed that all the samples exhibit high surface areas of 242.48 m^2/g, 231.14 m^2/g and 237.20 m^2/g. The slight decrease in the active surface for rGO-POMs sample is attributed to the inclusion of the POM nanoparticles, which contribute heavily to the total mass of the hybrid. Even with this slight decrease the specific BET surface areas of rGO-POMs are considerably larger than many recently reported carbon/metal oxide hybrid materials.[1, 2] Also, Chen et. al.[3] prepared a novel nanohybrid based on single-walled carbon nanotubes (SWCNTs) with a polyoxometalate $(TBA)_5[PV_2^{V}Mo_{10}^{VI}O_{40}]$ (TBA-PV_2Mo_{10}, TBA: $[(CH_3(CH_2)_3)_4N]^+$, tetra-n-butyl ammonium) and reported a maximum BET surface area of 71 m^2/g.

References

[1] Y. Ji, L. Huang, J. Hu, C. Streb, Y. F. Song, *Energy Environ. Sci.*, 2015, 8, 776-789

[2] W. Wei, X. Cui, W. Chen, D. G. Ivey, *Chem. Soc. Rev.*, 2011, 40, 1697-1721

[3] H. Y. Chen, R. Al-Oweini, J. Friedl, C. Y. Lee, L. Li, U. Kortz, U. Stimming, M. Srinivasan, *Nanoscale*, 2015, 7, 7934-7941.

Supporting information S3

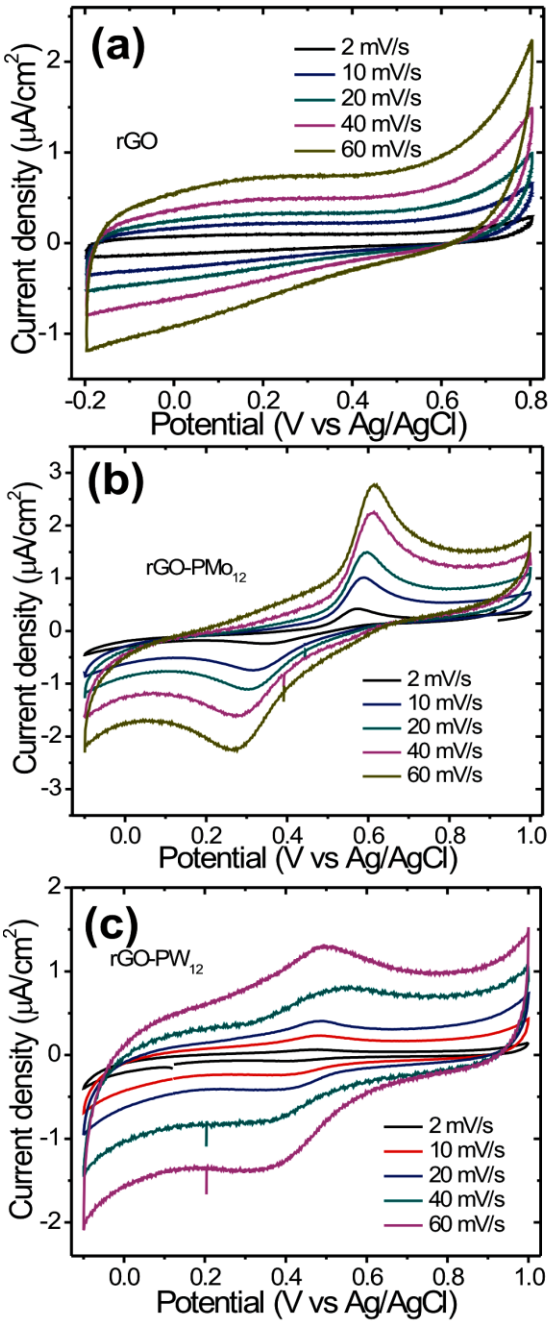

Figure S3 (a-c) CV curves of rGO, rGO-PMo_{12} and rGO-PW_{12} hybrid electroactive nanofluids with conventional three electrode set-up comprising glassy carbon, platinum wire and Ag/AgCl as working, counter and reference electrodes, respectively at different scanning rates.

Supporting information S4

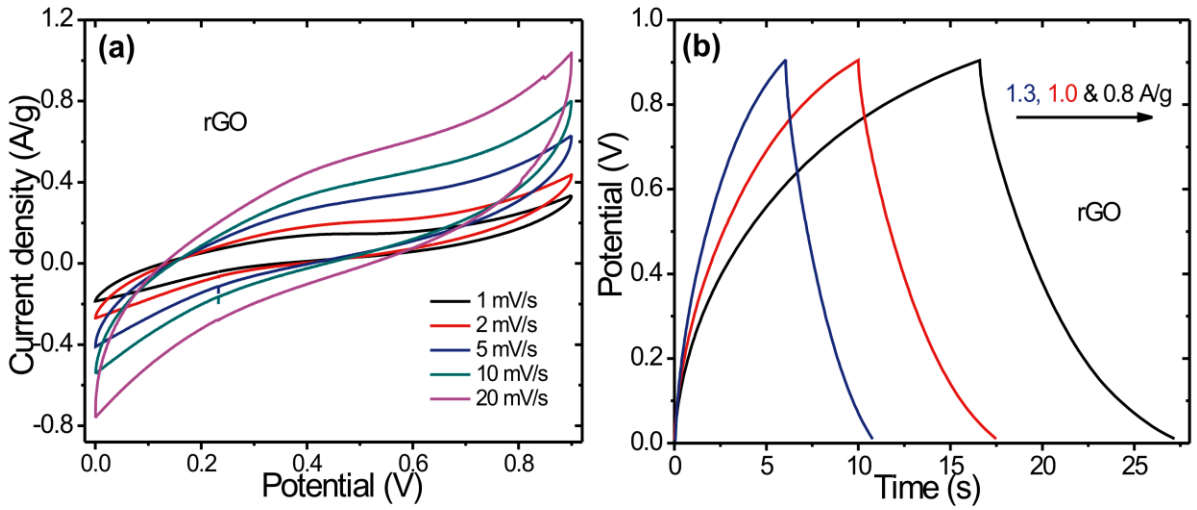

Figure S4 (a-b) Cyclic voltammetry and galvanostatic charge discharge curves of rGO nanofluids at different scanning rates and different current densities, respectively

Supporting information S5

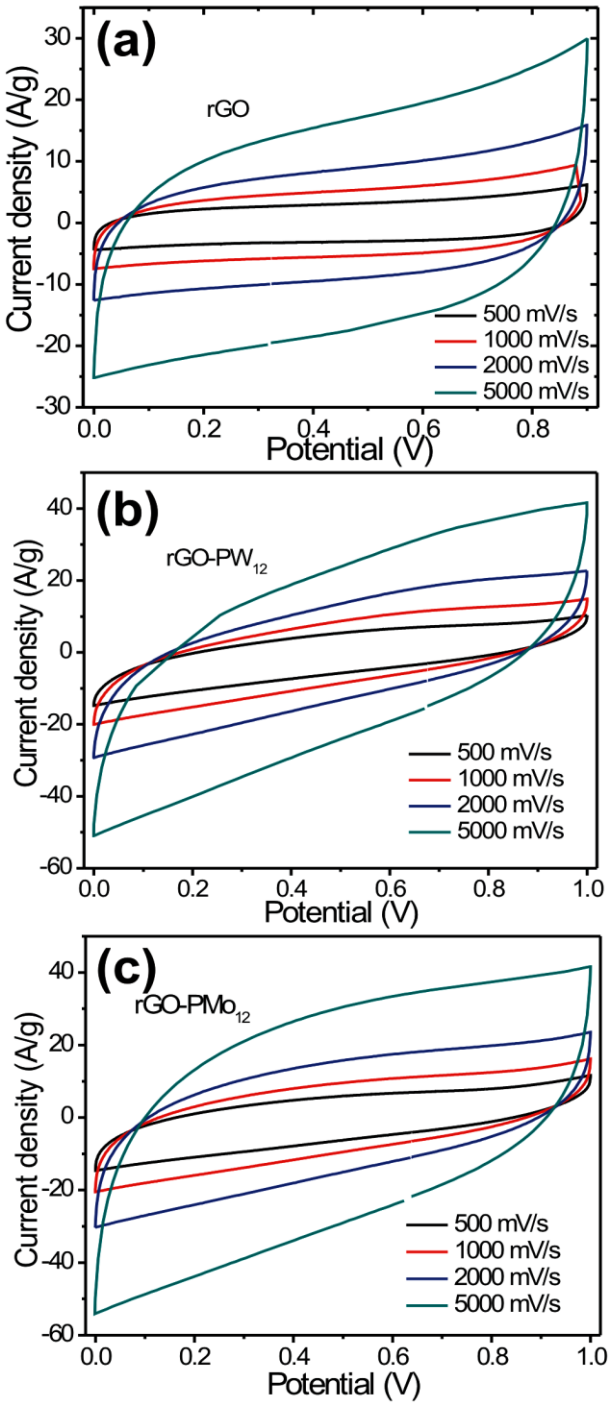

Figure S5 (a-c) Cyclic voltammetry curves of rGO, rGO-PW_{12} and rGO-PMo_{12} hybrid electroactive nanofluids at very high scan rates, respectively

Supporting information S6

Electrochemical parameters:

From cyclic voltammetry, the capacitance was calculated using the following equation:

$$C_{sp} = \frac{2\int idV}{v \cdot m \cdot \Delta E} \quad (1)$$

where Δ *E* is the voltage window, *i* the discharge current, *V* the voltage, *v* scan rate, and *m* the mass of rGO in one electrode. The factor of 2 accounts for the two electrode setup, where the charge is evenly distributed between two capacitors in series. Note that the specific capacitances were normalized by the mass of rGO in one electrode (not the total weight of nanofluids).

The specific capacitance C_{sp} was calculated from galvanostatic cycling using this equation:

$$C_{sp} = \frac{2i}{m \cdot \left(\frac{dV}{dt}\right)} \quad (2)$$

where *dV/dt* is the slope of the discharge curve.

Initially, the cell was discharged for 15 min (at 0 V) then the cell was charged to certain cell potential for 5 min and then discharged to 0 V for 5 min. Integration of the discharge curve directly yielded the charge of the two-electrode setup. The capacitance was extracted from the discharge curves of chronoamperometry experiments using the following equation:

$$C_{sp} = \frac{2\int idt}{m \cdot \Delta E} \quad (3)$$

The coulombic efficiency was determined according to the following equation and corrected for leakage current:

$$\varepsilon_C = \left|\frac{\int I_{discharge} dt}{\int I_{charge} dt}\right| \cdot 100\% \quad (4)$$

Supporting information S7

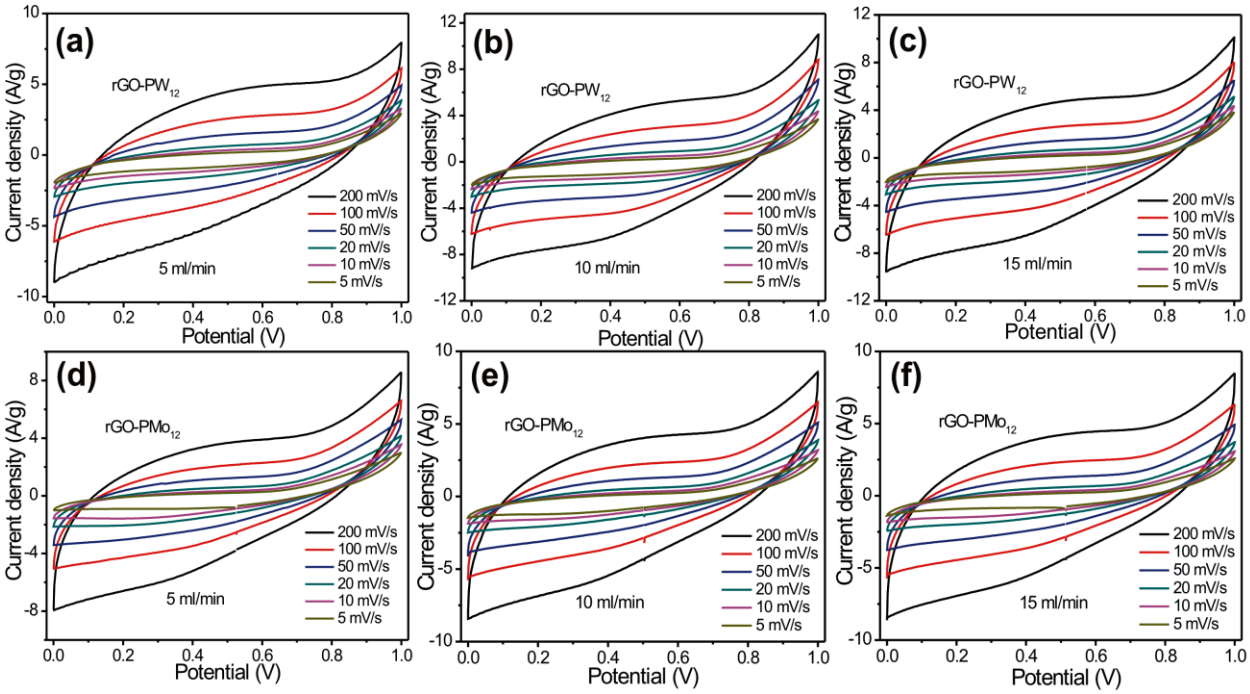

Figure S7 CV curves for (a-c) rGO-PW_{12} and (d-f) rGO-PMo_{12} hybrid electroactive nanofluids (HENs) at different scan rates for different flow rates (5 ml/min, 10 ml/min and 15 ml/min), respectively.